Heat Transfer Around a Tube in In-Line Tubes Bank Near a Plane Wall

Shinya AIBA, Yuichi SASAKI* and Tsutomu ITO*

(昭和 63 年 10 月 19 日受理)

Introduction

A large number of studies have been carried out concerning to the features of flow and heat transfer around tubes of in-line tube banks under the uniform flow field [1—5]. However, it is considered that all tubes of them are not always situated in the uniform flow field in practice. From this stand point, the present author have clarified the heat transfer characteristics around a single circular cylinder placed in the plane wall, as a first step [6].

In the uniform flow, behaviors of heat transfer around the tubes of in-line tube banks are quite different from those of a single cylinder [3—5]. Even the results of the first cylinder (also, the second cylinder) composed of four circular cylinders show a quite complicated variation with the in-line pitch, though it is generally accepted that the heat transfer of the tube in the first row of the tube bank is similar to that of a single cylinder. However, the average heat transfer results of the third cylinder and fourth cylinder are not so influenced by the in-line pitch, if the pitch is not smaller than the critical one indicated as follows:

$$(p/d)_c = 7.34\ Re^{-0.171} \qquad (1)$$

for the ranges $Re=10^4 \sim 5\times10^4$ and $p/d=1.15 \sim 3.4$, where p and Re are the pitch between cylinder's centers and Reynolds number based on the cylinder diameter d, respectvely [5]. The critical pitch ratio $(p/d)_c$ increases with decreasing Re. At a given value of p/d, the heat transfer rate of all four cylinders is lower than that of the single cylinder in the range of $p/d < (p/d)_c$.

The objective of the present study is to clear the heat transfer characterestics of tube banks in a cross-flow of air near the plane wall by investigating these of the third cylinder of four cylinders aligned at equal intervals, comparing with the results of the single cylinder and four cylinders in the uniform flow fields.

Nomenclature

c = distance between the cylinder and the plane wall
$C_p = (P-P_\infty)/(1/2)\rho U_\infty^2$ = static pressure coefficient
d = cylinder diameter
Nu = Nusselt number
P = static pressure
p = longitudinal spacing between cylinders' center
$Re = U_\infty d/\nu$ = Reynolds number
U = flow velocity
$\sqrt{\overline{U'^2}}/U_\infty$=stream turbulence intensity

* Former students

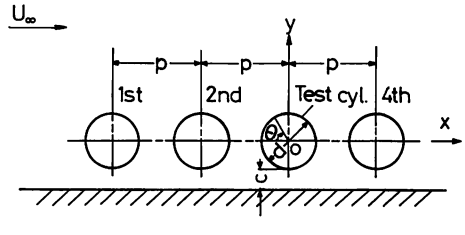

Fig. 1 Arrangement of cylinders and coordinate system

δ = thickness of the boundary layer
θ = circumferential angle from geometric forward stagnation point
λ, ρ, ν = thermal conductivity, kinematic viscosity and density of air at T_∞
Subscripts
m = mean
max = maximum
w = wall
∞ = undisturbed uniform stream

Exeperiments and procedures

The wind tunnel used in the present study is the same as that employed in previous studies [4—6], and the test section is a rectangle 325mm high and 225mm wide. The working section was devided by a horizontal partition plate mounted in the tunnel. The plate was 1000 mm long and 5 mm thick and had a round leading edge. Trip wire of diameter 1.4 mm was fixed across the plate 100mm from the leading edge. The free-stream turbulence of upstream uniform flow $\sqrt{\overline{U'^2}}/U_\infty$ was about 0.7 percent through the experiments. A constant-temperature hot wire anemometer with a single tungsten wire of 0.005 mm diameter as the sensing element was used for measuring the distribution of the velocity and turbulence intensity in the flow field around the test section.

Four cylinders spanned the wind tunnel horizontally as shown in Fig. 1(which also shows the coordinate system employed). The test cylinder (the third one) was placed at 750 mm downstream of the leading edge of the plate. Thickness of the turbulent boundary layer at the test cylinder position (but with the all four cylinders removed from the tunnel) was equal to about 21 mm. The boundary layer velocity distribution obtained agrees with that shown by Schubouer and Klebanoff [7]. It was also confirmed that the distribution of turbulence intensity on the wall at the test cylinder position was almost identical with that presented by Klebanoff [8].

Four cylinders were settled at equal intervals and were 15mm in diameter. The clearances between the cylinders and the plate were 0.75, 2.7, 5.7, 9.15, 12, 15, 18.5 and 60mm. In order to measure the clearance accurately a block gauge was used for all experiments. The in-line pitch ratio p/d was varied from 1.2 to 4.4 and the Reynolds number Re based on the cylinder diameter and undisturbed uniform flow velocity from 0.8×10^4 to 4×10^4.

For the heat transfer measurement of the test cylinder, a stainless steel ribbon wound helically around the center section of a plexiglass tube was electrically heated. The inside of the tube was filled with rigid urethane foam in order to minimize the heat loss by conduction. The correction of the loss by conduction in the radial direction amount to less than 1 percent of the electric power input. The wall temperatures were measured with 0.065 mm copper-constantan thermocouples affixed to the back of the stainless sheet at intervals of 10 deg. The maximum temperature of the test cylinder surface was kept under 38°C to reduce the radiative heat loss as much as possible. The heat loss by radiation from the cylinder surface was estimated to be about 0.6 percent of the heat supplied to the cylinder. Thus the present data were obtained under the condition of constant heat flux (the heat flux q to the test cylinder was ranged from 1.0 to 2.7 kw/m^2). The local heat transfer coefficient and the corresponding Nusselt number are defined, respectively, as follows:

$h_\theta = q/(T_w-T_\infty)$; $Nu_\theta = h_\theta d/\lambda$

In addition, three dummy cylinders were unheated during the heat transfer measurements.

Measurements of the wall static pressure were made using another cylinder which had

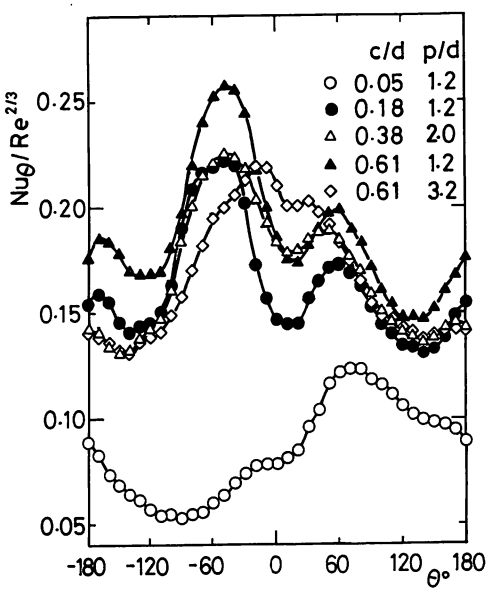

Fig. 2 Variation of local Nusselt number for Re ~3.4×10^4

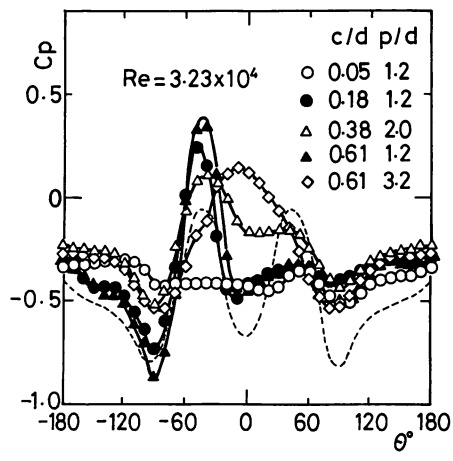

Fig. 3 Variation of local static pressure with c/d, p/d
(------; c/d=∞, p/d=1.2, Re=6.7×10^4 [2])

pressure hole of 0.5 mm diameter without heating at intervals of 10 deg. Oil flow patterns show the flow field to be two dimensional.

Experimental Results and Discussion

Local heat transfer characterestics. The typical distributions of the local Nusselt numbers Nu_θ are presented in Fig.2. The results have been shown as $Nu_\theta/Re^{2/3}$ at around $Re=3.4\times10^4$ considering that the average Nusselt number in the turbulent wake region is proportional to $Re^{2/3}$. In the case of c/d=0.05, the maximum Nusselt number, Nu_{max}, occurs on the upper surface of the cylinder (θ =0～+180°). Although Nu_{max} locates in the vicinity of θ=75° for p/d=1.2 as shown in figure, it shifts upstream with increasing p/d. However, the result of c/d=0.18 is quite different from that of c/d=0.05, though the pitch ratio p/d is equal to 1.2. The heat transfer rate around cylinder levels up drastically comparing with that of c/d=0.05. And, it can be observed that Nu_{max} locates on the lower surface of the cylinder (θ = 0 ～ −180°) at around θ=−55°. That peak of Nu_θ is considered to be related to the reattachment of the free shear layer shed from the lower surface of the second cylinder. The behavior of this layer is strongly affected by the plane wall mentioned later. Another peak of Nu_θ at around θ=60° is resulted from the reattachment of the free shear layer shed from the upper surface of the second cylinder. However, this value of Nu_θ is smaller than that of Nu_{max}, and they agree with each other with increasing c/d. In the case of c/d=0.61 for the same pitch ratio p/d=1.2, the heat transfer rate around cylinder increases more than that of c/d=0.18.

These results may show that the heat transfer phenomena treated herein are closely related to the clearance between the cylinders and the plane wall. For c/d=0.61 Nu_{max} locates at around θ=−20° when the pitch ratio increases such as p/d=3.2 shown in the figure, and the another peak, which exists in the neighborhood of θ=+30°, is not clear.

Shinya AIBA, Yuichi SASAKI*and Tsutomu ITO*

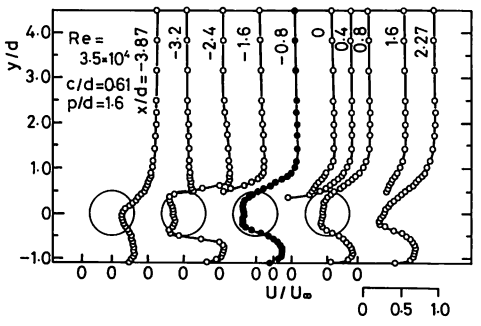

Fig.4 Distribution of velocity over the test field

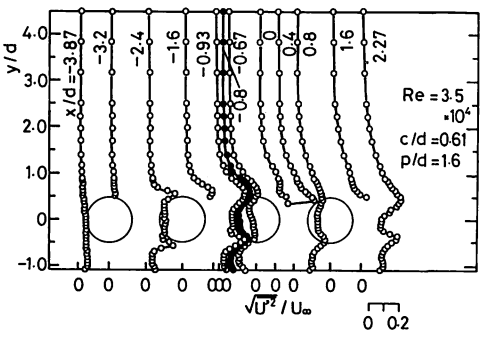

Fig. 5 Distribution of turbulence intensity over the test field

In general, it can be said that variations of Nu_θ around the cylinder decrease with increasing p/d, when c/d equals to a constant (see Fig.6 also). These trends may be related to the variations of the free shear layers shed from the second cylinder.

The distributions of pressure coefficient C_P corresponding to the same conditions in Fig.2 are shown in the figure 3 for $Re=3.23\times10^4$. In the figure, the result of Eastop and Turner [2] indicated by dotted line is included also, which was obtained under the conditions of $c/d=\infty$, $p/d=1.2$ and $Re=6.7\times10^4$.

The distribution of C_P for c/d=0.05, p/d=1.2 changes little around the cylinder comparing with other results. It can be considered that the flow around the cylinder is very stagnant in this case and Nu_θ becomes to small as shown in Fig.2. In the results for c/d=0.18, 0.61 except the case p/d=3.2, there exist sharp peaks in the vicinity of $\theta=-45\sim-50°$. These

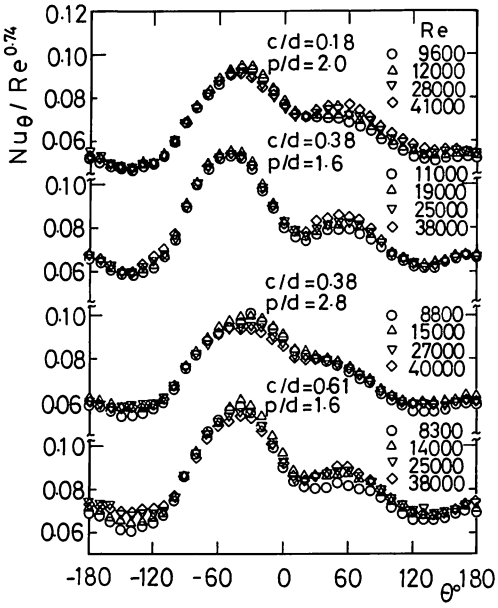

Fig. 6 Local Nusselt number distribution with Reynolds number

C_{pmax} are larger than the result of uniform flow field obtained by Eastop and Turner. Another peak's values of C_P on the upper surface of the cylinder are smaller than the results of the lower surface, and the locations of these peaks are not always clear. These results may show that the free shear layer shed from the lower surface of the second cylinder is deflected to the upward (say, y direction) by the existence of the plane wall, and the upper side free shear layer shed from the second cylinder is also deflected to the y direction. As a result, it may be considered that the relative slow velocity flow in the upperside shear layer reattaches to these locations, in view of the flow field measurements.

In the case of p/d=3.2, C_{pmax} locates at around $\theta=-10°$. This indicates that the free shear layer of the plane wall side may be rolled up towards the front surface of the cylinder. Figure 4 indicates the velocity distributions of the flow field in the case of c/d=0.61, p/d=1.6 and $Re=3.5\times10^4$. The velocity profile of x/d=−0.8, where is the center section between the second

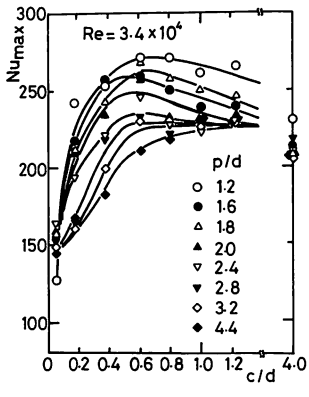

Fig. 7 Corelation of Nu_{max} with c/d, p/d

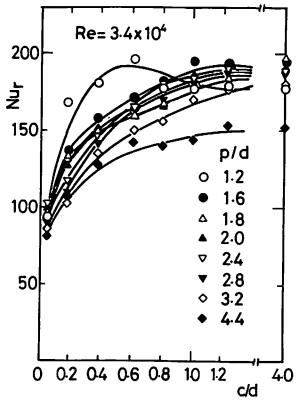

Fig. 8 Corelation of Nur with c/d, p/d

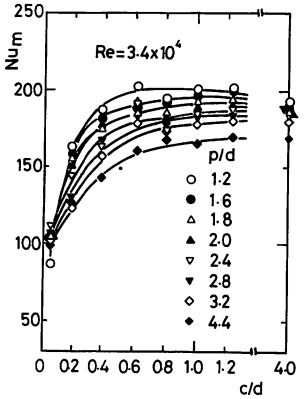

Fig. 9 Variation of Nu_m with c/d, p/d

cylinder and the test one, is similar to that of x/d=0.8, though the velocity gradients of the shear layers to the perpendicular to the main flow direction are relatively larger than these of x/d=0.8. From this, it is assumed that the behavior of heat transfer of the fourth cylinder may be identical with that of the test cylinder [9]. It can be seen also from the profile of x/d=−0.8 that the velocity gradient of the shear layer in the range $y/d<0$ is larger than that for $y/d>0$. Where the velocity gradient of the shear layer is large, the turbulnce intensity takes large value and in the neigborhood of the most large velocity gradient it occurs maxima as shown in the figure 5. These peaks of the turbulent intensity in the section of x/d=−0.8 can be seen at y/d=0.58 and −0.43. From these results, it may be considered that the occurence of Nu_{max} of the lower surface of the cylinder is resulted from the reattachment of the relative large velocity part of the shear layer with the high turbulence intensity, considering also the results of other sections between the second cylinder and the test one. And it may be confirmed that the flow velocity of the shear layer which reaches to the upper surface is smaller than that to the lower surface.

In spite of the problems of measurement in such flow fields, the hot wire anemometer is possibly useful one in order to examine qualitatively the relation between the heat transfer and the flow [4].

The distributions of Nu_θ versus Reynolds number have been described in Fig.6. The results are summarized as $Nu_\theta/Re^{0.74}$, because the average Nusselt number is proportional to $Re^{0.74}$ as shown in Fig. 12 in the ranges c/d=0.18∼0.61, p/d=1.2∼3.2. It can be seen that the local Nusselt number at any angular position is approximately proportional to $Re^{0.74}$ within an average discrepancy of 5 percent.

Figures 2 and 6 show that Nu_{max} in the lower surface play an important role for the average Nusselt number Nu_m around the cylinder. Therefore it is important to know the features of Nu_{max}. Figure 7 illustrates the variations of Nu_{max} against c/d with p/d for $Re=3.4\times10^4$. In the case of c/d=0.05 (Nu_{max} locates at the upper side of the cylinder independent of p/d and Re in this case), the results are influenced little by p/d except that of p/d=1.2. In the range $c/d>0.05$, it is confirmed that Nu_{max} increase abruptly with increasing c/d and are relatively influenced by p/d. However, for $c/d\geqq0.5\sim0.6$ the increasing ratio of Nu_{max} versus c/d seems to decrease, and for $p/d\leqq2.8$ Nu_{max} rather decrease with increasing c/d. Moreover, it can be found that Nu_{max} has large values as p/d is small for $c/d<0.61$ except the case of c/d=0.05. However, they are not so much influenced by p/d with inceasing c/d as seen in the case of c/d=4.0.

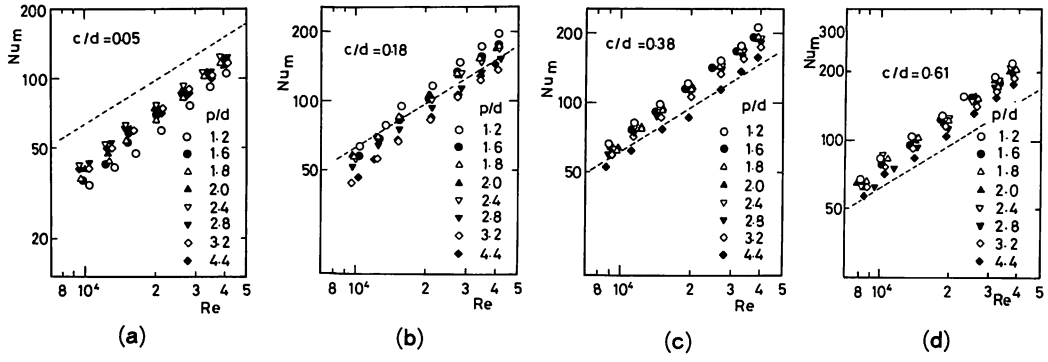

Fig. 10 Variations of mean Nusselt number for Re: (a) c/d=0.05; (b) c/d=0.18; (c) c/d=0.38; (d) c/d=0.61;--------, result of single cylinder in the uniform flow field

In order to show the heat transfer characterestics of the rear face of the cylinder, the variations of the Nusselt number of $\theta=180°$, Nu_r, are presented in Fig.8. Nu_r have the same trend of the Nu_{max} which increase with increasing c/d for c/d$<$0.61, though Nu_r do not vary so abruptly with c/d as the cases of Nu_{max} except for c/d=1.2. For c/d$\geqq$0.61, increasing ratios of Nu_r for c/d decrease, and especially the results of p/d=1.2 somewhat level down.

Mean heat transfer characteristics. Figure 9 shows the results for mean Nusselt number with c/d for at around $Re=3.4\times10^4$. From this it can be seen that they increase monotonically with increasing c/d for c/d$<$0.61 and the increasing ratios of Nu_m for c/d$>$0.61 decrease (Nu_m rather change little with c/d). In the case of c/d=0.05, p/d does not play an important role in the behavior of Nu_m except for p/d=1.2. The same trends can be seen in the case of c/d=4.0 except for p/d=4.4. They had been observed also in the previous work in the uniform flow field [9]. In that field, the critical in-line pitch ratio $(p/d)_c$ defined by eq.(1) is equivalent to 1.23 for $Re=3.4\times10^4$ and the critical Reynolds number for p/d=1.2 is 3.9×10^4. Therefore the results for p/d=1.2 in the range $Re<3.9\times10^4$ must be lower than those for p/d$\geqq$1.6 in the uniform flow field.

While, it is obvious that the results shown in the Fig.9 are different from these in the uniform flow field for c/d$>$0.05. This difference may be resulted from the flow structure which is rolled up to the front face of the cylinder being deflected by the existence of the plane wall, despite the small pitch ratio such as p/d=1.2. In the range c/d=0.18$\sim$1.23, Nu_m generally increase with decreasing p/d (that is, $Nu_m \propto (p/d)^{-0.12}$ as shown in Fig.11).

In order to show the dependency of Nu_m for Re, the results are illustrated in the Fig.10 for c/d=0.05, 0.18, 0.38 and 0.61, respectively. It is found that the trends of Nu_m shown in Fig.9 do not change by the Reynolds number treated in this study. The results of c/d=0.05 are smaller about from 30 to 45 percent in maximum than that of the single cylinder in the uniform flow field indicated by the dotted line. For c/d=0.18, they are smaller than those of the dotted line also in the range $Re<1.4\times10^4$, independent of p/d. And, they become larger than that of the single cylinder for p/d$<$2.8, when $Re>2\times10^4$. For the both cases of c/d=0.38, 0.61, Nu_m are not smaller than these of the single cylinder except the case of p/d=4.4, in the range $Re=0.8\times10^4\sim4\times10^4$, and the increasing ratios of Nu_m increase with increasing Reynolds number (for p/d=1.2, the values of the Nu_m become about 1.5 those for the single cylinder in the uniform flow field for $Re=4\times10^4$).

In view of the fact that the average Nusselt numbers are inversely proportional to $(p/d)^{0.12}$ as already noted, the results of $Nu_m(p/d)^{0.12}$ are demonstrated as a function of c/d in Fig.11. It

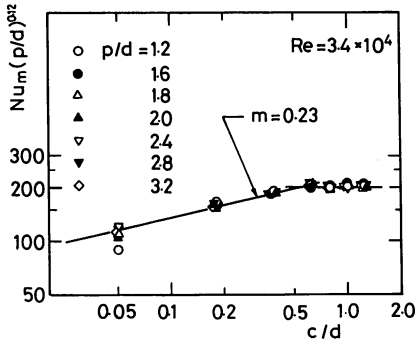

Fig. 11 Corelation of $Nu_m (p/d)^{0.12}$ for c/d

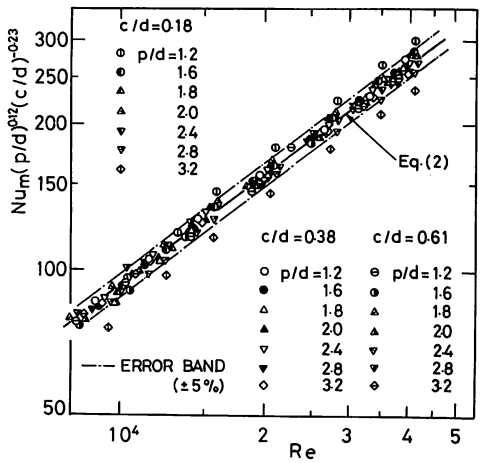

Fig. 12 Mean Nusselt number results

appears that the data are better correlated in the ranges c/d=0.18～1.23 and p/d=1.2～3.2. In the range of c/d=0.18～0.61, $Nu_m(p/d)^{0.12}$ increase with increasing c/d and they are connected following relation; $Nu_m(p/d)^{0.12} \propto (c/d)^{0.23}$. As already shown in figure 10, the dependency of Nu_m for Re is almost linear independent of c/d.

Considering these facts, the data of $Nu_m(p/d)^{0.12}(c/d)^{-0.23}$ are ploted for those of c/d=0.18, 0.38 and 0.61 as a function of Reynolds number in Fig.12. The data displayed in this figure are good correlated against Reynolds number within a ±5 percnt error band of following equation (2) except those for c/d=0.18, p/d=1.2 and 3.2. The equation of the fitted line is

$$Nu_m = 0.103\ (p/d)^{-0.12}\ (c/d)^{0.23}\ Re^{0.74} \qquad (2)$$

in the ranges $Re=0.8\times10^4$～4×10^4, c/d=0.18～0.61 and p/d=1.2～3.2. However, the data for the cases of c/d=0.18, p/d=1.2 are somewhat larger than the results predicted by the equation (2) in the range $Re>1.5\times10^4$, and the data for the cases of c/d=0.18, p/d=3.2 are lower than those obtained by eq. (2) about 12～15 percent independent of Reynolds number. In the cases of c/d=0.18, p/d≧3.2, the distributions of Nu_θ are similar to that for c/d=0.05 as shown in Fig.2. Furthermore, the results of mean Nusselt number Nu_m in the range 0.61<c/d≦1.23 are relatively independent of c/d as foregoing, and there exist a corelation of such as $Nu_m \propto Re^{0.73}$ (the power of Re is somewhat smaller than that for c/d≦0.61).

Concluding Remarks

Heat transfer around the third cylinder of four cylinders aligned in-line in cross flow of air near a plane wall have been investigated as the functions c/d, p/d and Re. When c/d is very small such as c/d=0.05, Nu_{max} occurs on the upper surface of the cylinder and the Nu_θ around cylinder is lower than that for c/d>0.05 independent of p/d resulted from the stagnation of the flow around the cylinder. Nu_θ takes maximum values on the lower surface of the cylinder (except the special cases such as c/d=0.05, and c/d=0.18, p/d=3.2) influenced by the free shear layer shed from the second cylinder which is deflected by the existence of the plane wall. Nu_m increases monotonically with c/d in the range c/d=0.05～0.61, and changes little by c/d for c/d>0.61 (Fig.9). Though p/d does not play an important role for Nu_m than c/d, it must be noticed that Nu_m is inversely

proportional to p/d except for the case c/d=0.05.

A correlation of the all over the heat transfer yielded the compact expression $Nu_m=0.103(p/d)^{-0.12}(c/d)^{0.23}Re^{0.74}$, with a spread of ±5 percent in the ranges c/d=0.18～0.61, p/d=1.2～3.2, and $Re=0.8\times10^4$～4×10^4, except the case for c/d=0.18, p/d=3.2.

References

1 Zdravkovich, M, M., Trans. J. Fluids Engng., 99—4 (1977), 618.
2 Eastop, T.D., and Turner,J.R.,Trans. IChemE, 60 (1982), 359.
3 Kostić,Z.G., and Oka,S.N., Int. J. Heat Mass Transfer, 15—2 (1972), 279.
4 Aiba,S., and Yamazaki,Y.,Trans. ASME, J. Heat Transfer, 98 (1976), 503.
5 Aiba,S.et al., Int. J. Heat Mass Transfer, 33 (1980), 311.
6 Aiba,S.,Trans.ASME,J. Heat Transfer, 107 (1985), 916.
7 Schubauer,G.B., and Klebanoff,D.S., NACA TR No. 1289, 1956.
8 Klebanoff,P.S., NACA TR No. 1247, 1955.
9 Aiba,S.et al., Bull.of the JSME, 24—188 (1981), 380.